Dandelion Extract Relaxes Mouse Airway Smooth Muscle by Blocking VDLCC and NSCC Channels

zhao ping (p.zhao@scuec.edu.cn)
South-Central University for Nationalities https://orcid.org/0000-0002-5348-6126
Jia Liu
south-central university for nationalities
Qian Ming
south-central university for nationalities
Di Tian
south-central university for nationalities
Jingwen He
south-central university for nationalities
Ziwei Yang
south-central university for nationalities
Jinhua Shen
south-central university for nationalities
Qinghua Liu
south-central university for nationalities
Xinzhou Yang
south-central university for nationalities

Research

Keywords: Ethyl acetate extract from dandelion; Airway smooth muscle; Relaxation; Ca2+; Ion channels

Posted Date: July 13th, 2020

DOI: https://doi.org/10.21203/rs.3.rs-22992/v2

Version of Record: A version of this preprint was published on October 28th, 2020. See the published version at https://doi.org/10.1186/s13578-020-00470-8.

Abstract

Background: Asthma is one of the main intractable diseases recognized by the international medical community. The current widely used bronchodilators for asthma—β2-adrenal receptor agonists—have limited therapeutic effects, necessitating the development of novel antiasthma drugs with increased efficacy and fewer adverse effects. In this study, we investigated the relaxant effects and underlying mechanism of an ethyl acetate extract from dandelion (EAED) on mouse airway smooth muscle.

Methods: The effects of EAED on agonist-induced precontraction in mouse airway smooth muscle were evaluated with force measurement. Mouse lung slices were used to study the effects of EAED on bronchial smooth muscle. The intracellular Ca^{2+} concentration was measured using a calcium imaging system. L-type voltage-dependent calcium channel (VDLCC) and non-selective cationic channel (NSCC) currents were measured by patch-clamp. The lung functions of healthy and asthmatic mouse groups were assessed via the forced oscillation technique.

Results: EAED inhibits acetylcholine-induced sustained contractions of whole airway smooth muscle by inhibiting VDLCCs, NSCCs, and some unknown channels, reduces the agonist-induced increase in the cytosolic free Ca^{2+} concentration in airway smooth muscle cells, blocks VDLCC and NSCC currents, and relieves the respiratory resistance of healthy and asthmatic mice.

Conclusions: EAED may have potential beneficial effects on asthma attacks.

Background

Asthma, as a major chronic respiratory disease, threatens the health of hundreds of millions of people around the world [1]. The consultation and mortality rates of asthma patients are increasing year by year [2]. Airway inflammation, airway hyperresponsiveness, and airway remodeling are important pathophysiological characteristics of asthma. Airway smooth muscle (ASM) is the key tissue regulating airway resistance, hyperreactivity, and contraction, the major features of asthma [3]. ASM cells (ASMCs) are an important cell type in ASM and excessive contraction of ASMCs leads to the development of asthma symptoms by narrowing the airway lumen and limiting gas exchange [3]. ASM contraction induced by agonists (*i.e.* acetylcholine, 5-hydroxytryptamine) usually relies on an increase in $[Ca^{2+}]_i$ and on Ca^{2+} oscillations. These oscillations are caused by the release of Ca^{2+} from the intracellular calcium pool and the influx of Ca^{2+} from the extracellular space [4].

The first-line treatment for asthma is still a combination of β_2 adrenergic receptor agonists and glucocorticoids. However, this therapeutic strategy can have severe adverse effects, such as headache, tremors, palpitations, and heart failure. Thus, in this study, we attempted to develop a safe and effective plant-based drug to inhibit ASM contraction.

Dandelion is a perennial herbaceous plant with the scientific name *Taraxacum mongolicum* Hand. -Mazz. (TMHM) that belongs to the composite family. Its main chemical components are taraxasterol, choline, organic acid, inulin, and other healthy nutrients [5]. It is thus often eaten as a nutritious wild vegetable. In addition, it has many pharmacological effects. Modern pharmacological studies show that the properties of dandelion include antibacterial [6, 7], antiviral [8], anticancer [9-13], antioxidant [14], anti-inflammatory [15-17], and antiallergic functions. In terms of the alleviation of airway inflammation, a distinctive feature of asthma, it has been reported that the organic acid components of TMHM can improve lipopolysaccharide-induced histopathological damage to tracheal tissues [18] and reduce lipopolysaccharide-induced inflammation in normal human bronchial epithelial cells [19], which could be beneficial for the treatment of acute tracheobronchitis. Taraxasterol was also found to be effective in improving ovalbumin-induced allergic asthma in mice [20]. Abundant literature also concerns the potential efficacy of dandelion in mice. However, no studies have examined whether a specific component from dandelion has the potential to inhibit mouse ASM contraction.

In this study, we found that EAED exerted inhibitory effects on mouse ASM precontraction and investigated the underlying mechanism.

Methods

Dandelion Extraction

Dandelion was purchased from Beijing TongrenTang (Wuhan, China). The air-dried dandelion (0.5 Kg) was milled into powder and soaked in 80% ethanol (5L) for 3 days. Then the crude ethanol extract was obtained by filtration and rotary evaporation. The ethyl acetate extract of dandelion was obtained by phase separation extraction. The dried ethyl acetate extract of dandelion was dissolved in 3% DMSO for the experiments.

Reagents

Nifedipine, acetylcholine chloride (ACH), and pyrazole3 (Pyr3) were purchased from Sigma Chemical Co. (St. Louis, MO, USA); Fura-2 AM were purchased from Invitrogen (Eugene, OR, USA). Other chemicals were purchased from Sinopharm Chemical Reagent Co. (Shanghai, China).

Animals and Establishment of asthma model mice

Six-weeks-old male BALB/c mice were purchased from the Hubei Provincial Center for Disease Control and Prevention (Wuhan, China) and were housed in a specific pathogen free (SPF) grade animal facility. All animal experiments were performed in accordance with the requirements of the Institutional Animal Ethics Committee of the South-Central University for Nationalities. The license number is 2016-SCUEC-AEC-0030. Asthmatic mice were prepared as described previously [21]. And, the mice were sacrificed with an intraperitoneal injection of sodium pentobarbital (250 mg/kg, purity ≥ 98%; Sigma) before or after performing each experiment.

Contraction measurement of tracheal and bronchial ASM

Mouse ASM tension was measured as previously described [22]. Briefly, mouse TRs were clipped clean, cut about 1 cm and hung on the triangular hook in a 6 mL PSS bubbled with 95% O_2 and 5% CO_2 at 37°C. A 300 mg preload is set. TRs was equilibrated for 1 hour and then prestimulated with 100 μM ACH or 80 mM KCl for 20 minutes. After resting for another 20 minutes, experiments were performed.

ASM force measurements in mouse lung slices were performed as previously described . In brief, the lung slices were cut and placed in a chamber perfused using Hanks' balanced salt solution (HBSS). The LSM 700 laser confocal microscope and Zen 2010 software (Carl Zeiss, Göttingen, Germany) were performed to measure the cross-sectional areas of the bronchial lumen. Each part of the experiment was independently repeated for more than six times (i.e., more than six random mice).

Measurement of plasma calcium concentration in ASMCs

Mouse acute detached ASMCs suspension was diluted to an appropriate density and was treated with poly-D-lysine. A specially designed cell bath of the passed slides is placed in an inverted microscope connected to the calcium imaging system. Poly-D-lysine could help cells adhere to the glass slide. Then cells were dyed with 2.5 M fura-2 AM color. After 20 minutes of staining, PSS physiological saline solution was perfusion for 5 minutes to wash away the excess fura-2. With calcium imaging TILL imaging system: 340 and 380 fluorescence images of the cell area, Ratio (340/380) can be used to reflect the intracellular calcium concentration. Each part of the experiment was based on more than 30 ASMCs (i.e., more than six random mice).

Patch

VDLCCs and NSCCs currents induced by ACH were recorded using EPC-10 patch clamp amplifier (HEKA, Lambrecht, Germany) and utilizing whole-cell recording mode. VDLCCs current was stimulated by step voltage from - 70 mV to + 40 mV. NSCCs current was recorded with nifedipine, niflumic acid and TEA in the solution in advance, under the condition of the ramp, voltage from - 80 mV to + 60 mV in 500 ms. Each part of the experiment was independently repeated for more than six times (i.e., more than six random ASMCs/mice).

Pulmonary function measurement

Lung function of groups of healthy or asthmatic mice were measured using forced oscillation technique (FOT). Mice were weighed and anesthetized with an injection of sodium pentobarbital (10 mg/kg, ip). After complete anesthesia, the mice were intubated and placed in a flow-type body plethysmograph and connected via the endotracheal cannula to a flexiVent system (SCIREQ Inc., Montreal, Canada). Lung function was assessed subsequently by FOT at baseline and following multiple concentrations of aerosolized ACH (3.125 - 50 mg/mL) dissolved with vehicle or EAED. Respiratory system resistance (Rrs) were calculated in the flexiVent software to reflect the degree of airway hyperresponsiveness. Each part of

the group experiment was independently repeated for more than six times (i.e., more than six random mice).

Data analysis

The results are expressed as mean ± SEM. Comparisons between two groups were performed with Student's t-test using Origin 9.0 software (OriginLab, Northampton, USA). Differences with p□0.05 were considered significant.

Results

EAED inhibits tracheal ring contraction

We first studied the effects of EAED on tracheal ring (TR) contraction. TRs were precontracted with 80 mM KCl and EAED was added when the contraction reached a plateau. The contraction was inhibited in a dose-dependent manner (Figure 1A). As a comparison, vehicle (PSS containing 3% DMSO), which was used to dissolve the EAED, was added at the same doses when the contraction stabilized (Figure 1B) and no relaxation was detected. This suggests that EAED indeed relaxes ASM. The half-maximal inhibitory concentration (IC_{50}) of EAED was 0.063 ± 0.005 mg/mL (Figure 1C). We also found that the contraction induced by 80 mM KCl was almost completely inhibited at an EAED concentration of 1 mg/mL. These results were obtained from 7 TRs from 7 mice.

Figure 1. EAED inhibited high K^+-induced TR contraction. (A) K^+ (80 mM) induced a sustained contraction in mouse TR, which was blocked by EAED in a concentration-dependent manner. The dose-inhibition curve is presented. (B) Similar experiments were performed with vehicle (PSS containing 3% DMSO) as control. (C) The dose-inhibition curve is presented. The IC_{50} of EAED was 0.063 ± 0.005 mg/mL. The data were obtained from 7 TRs.

Similarly, EAED was added after the contraction arising from 100 μM ACh) peaked, which induced a gradual but clear inhibition of the precontracted TRs (Figure 2A). In addition, vehicle control (PSS containing 3% DMSO) was added at the same doses under steady contraction conditions (Figure 2B), which again exerted no relaxant effects. Analysis of the dose-relaxation relationships determined an IC_{50} of EAED of 0.139 ± 0.04 mg/mL (Figure 2C). The EAED concentration inducing maximum relaxation was 3.16 mg/mL. These experiments indicated that EAED could block high K^+- and ACh-induced TR precontraction. In addition, the addition of 3.16 mg/mL EAED without pretreatment with any agonist resulted in a small immediate contraction and a subsequent return to baseline (Figure 2D), which indicated that EAED had no effect on the TRs in the resting state.

Figure 2. Contraction induced by ACh (100 μM) was inhibited by cumulative addition of EAED. (A) ACh induced a sustained contraction of TRs, which was inhibited by cumulative application of EAED. (B) Similar experiments were conducted but with vehicle (PSS containing 3% DMSO) as control. (C)

Summary of the results of the EAED-induced relaxation in 7 TRs. The IC_{50} of EAED was 0.139 ± 0.04 mg/mL. (D) EAED had no effect on the basic tone of ASM.

EAED blocks bronchial smooth muscle contraction

To investigate whether EAED has a similar relaxant effect on mouse bronchial smooth muscle, the effects of EAED on lung slices were examined. Treatment with 100 μM ACh decreased the tracheal cavity area; the addition of EAED restored the lumen area (Figure 3A). A summary of the data from 6 lung slices from 5 mice is shown in Figure 3B. After the addition of 100 μM ACh for 40 min, the area of the lumen reduced to approximately 48%; subsequent application of 3.16 mg/mL EAED for 120 min further decreased the area by about 82% reduction compared with the initial value. These results suggested that EAED may also inhibit the contraction of bronchial smooth muscle.

Figure 3. EAED inhibits contraction in lung slices. (A) The airway lumen area in a lung slice was decreased by ACh and was markedly increased by the addition of EAED. (B) Summary of the results obtained. Data were derived from 6 lung slices from 5 mice. *P < 0.05; **P < 0.01; ***P < 0.001.

EAED exerts diastolic effects by inhibiting L-type Ca^{2+}, TRPC3, and/or STIM/Orai channels

To investigate the mechanism of the EAED inhibition of ACh-induced contraction, 10 μM nifedipine, a selective blocker of voltage-dependent calcium channels (VDCCs), was added after contraction was induced by ACh (Figure 4A). The drug partially blocked the contractions, giving a relaxation value of about 18%. The remaining contractions were further blocked by EAED, with a relaxation of about 95% compared with baseline (Figure 4B). These data were obtained from 7 TRs of 7 mice.

Next, we investigated the nifedipine-resistant components of EAED-induced relaxation. Hence, TRs were incubated with 10 μM nifedipine for 15 min and ACh was then added. The effect of Pyr3 was observed. The overall results from 6 TRs of 6 mice showed that Pyr3 induced partial relaxation (about 25%; Figure 4C), with the remaining contractions completely blocked by EAED (almost 100%; Figure 4D).

Figure 4. Nifedipine and Pyr3 both partially inhibit ACh-induced contraction. (A) ACh (100 μM) induced the contraction of mouse TRs, which was partially inhibited by 10 μM nifedipine, with the remainder inhibited by 3.16 mg/mL EAED. (B) Summary of the results obtained from 7 TRs. (C) Mouse TRs were preincubated with 10 μM nifedipine. ACh induced TR contraction, which was partially blocked by Pyr3, with the remainder completely inhibited by 3.16 mg/mL EAED. (D) Summary of the results obtained from 6 TRs.

EAED inhibits Ca^{2+} influx induced by high K^+ and additional Ca^{2+} release induced by ACh

To further confirm the relationship between these channels and relaxation, a calcium-free and physiological calcium conversion experiment was designed. As shown in Figure 5A, when the TR was at 0 Ca^{2+}, high K^+ still activated the L-type voltage-dependent calcium channel (VDLCC) without increasing the

intracellular Ca^{2+} concentration. Thus, it could not cause TR contraction. When the extracellular $[Ca^{2+}]_i$ was returned to 2 mM, the extracellular Ca^{2+} flowed rapidly, the intracellular $[Ca^{2+}]_i$ increased, and the TR constricted. This contraction was inhibited by 1 mg/mL EAED. Furthermore, incubation with EAED almost completely abolished the contraction induced by 2 mM Ca^{2+} (Figure 5B). From these results, it can be concluded that EAED relaxation of precontracted tracheal smooth muscle induced by high K^+ was mediated by inhibition of VDLCCs and Ca^{2+} influx.

ACh can activate both VDLCCs and non-selective cationic channels (NSCCs), which leads to extracellular Ca^{2+} influx, release of Ca^{2+} from the sarcoplasmic reticulum into the cytoplasm, increased Ca^{2+} concentration, and ultimately contraction of tracheal smooth muscle. ACh was added under calcium-free conditions. Because there was no Ca^{2+} outside the cell, it caused a transient release of Ca^{2+} from the sarcoplasmic reticulum, leading to a transient contraction. When the extracellular $[Ca^{2+}]_i$ was restored to 2 mM, the Ca^{2+} in cytoplasm was increased by both the Ca^{2+} from the sarcoplasmic reticulum and the increase in extracellular Ca^{2+} (Figure 5C). Thus, the trachea showed a continuous and stable contraction. This contraction was inhibited by 3.16 mg/mL EAED. Moreover, under Ca^{2+}-free conditions (0 Ca^{2+} and 0.5 mM EGTA) in the presence of EAED, ACh did not induce a transient contraction. With the addition of 2 mM Ca^{2+}, only a very weak contraction occurred, which gradually returned to baseline (Figure 5D). These results indicated that EAED-induced relaxation was exerted through inhibition of the ACh-elicited Ca^{2+} influx and Ca^{2+} release.

Figure 5. EAED blocks high K^+-evoked Ca^{2+} influx and ACh-elicited Ca^{2+} influx and Ca^{2+} release. (A) A representative force tracing of 4 TRs. In the absence of calcium ions in the bath solution (0 Ca^{2+} and 0.5 mM EGTA), high K^+ could not cause TR contraction. When the calcium ion concentration was restored to 2 mM, a sustained and stable contractile reaction was produced, which was inhibited by the subsequent addition of EAED. (B) Identical experiments were performed as described in the presence of 1 mg/mL EAED, and high K^+-induced contraction did not appear after the restoration of 2 mM Ca^{2+}. (C) After nifedipine blockade of the VDLCC, ACh was added in the bath solution without calcium, and the TR exhibited instantaneous internal calcium release. After the calcium ion concentration recovered to 2 mM, the TR showed a stable contraction reaction, which could be completely inhibited by 3.16 mg/mL EAED, returning the TR contraction to the baseline level. (D) After pretreatment with 3.16 mg/mL EAED, the process of internal calcium release was significantly inhibited in a 0 Ca^{2+} and 2 mM Ca^{2+} conversion experiment, with the contraction reaction caused by ACh significantly inhibited when the calcium ion concentration was restored to 2 mM.

EAED inhibits Ca^{2+} elevation in single ASMCs

Next, the effects of EAED on intracellular Ca^{2+} in single ASMCs were examined by use of the TILL calcium imaging system. High K^+- (Figure 6A) and ACh- (Figure 6C) induced increases in intracellular Ca^{2+} were inhibited by 1 mg/mL or 3.16 mg/mL EAED. The 340/380 ratio at the sites indicated by a, b, and c were

obtained and a summary of the results from 30-35 cells of 5 mice are shown (Figure 6B and D). After the addition of high K^+, the 340/380 ratio increased from 0.51 ± 0.01 at point a to 0.75 ± 0.02 at point b, before reducing to 0.35 ± 0.01 at point c with the subsequent addition of 1 mg/mL EAED. Similar results were found with the ACh-stimulated increase in $[Ca^{2+}]_i$, where the 340/380 ratio increased from 0.44 ± 0.01 at point a to 0.55 ± 0.01 at point b, before reducing to 0.33 ± 0.01 at point c with the subsequent addition of 3.16 mg/mL EAED. These results suggest that the $[Ca^{2+}]_i$ decreases were due to inhibition of the above Ca^{2+}-permeant ion channels by EAED.

Figure 6. EAED inhibits high K^+- and ACh-induced Ca^{2+} increases in single tracheal smooth muscle cells. (A) A transient and sustained increase in intracellular Ca^{2+} was induced by 80 mM K^+. This increase was inhibited by the addition of EAED. The values were obtained at the sites indicated by a, b, and c. (B) Summary of the results from 35 cells of 5 mice. ***P < 0.001. (C) The increase in the calcium level in tracheal smooth muscle cells induced by ACh was inhibited by 3.16 mg/mL EAED. (D) Summary of the results from 30 cells of 5 mice. ***P < 0.001.

EAED effectively blocks VDLCC and NSCC currents

To further clarify the underlying mechanism, the currents regulated by VDLCCs and NSCCs were measured. As shown in Figure 7A, the VDLCC current was completely blocked by 10 μM nifedipine and 1 mg/mL EAED. The statistical data of 6 cells examined in each of the two experimental groups showed that +10 mV, 1 mg/mL EAED, and 10 μM nifedipine completely blocked the current.

To test whether EAED affects the opening of NSCCs, nifedipine, niflumic acid, and TEA were added to exclude the influence of VDLCC, K^+, and Cl^- currents, respectively. The results showed that the NSCC current was blocked by 3.16 mg/mL EAED under −70 mV voltage conditions (Figure 7B). These results indicated that EAED can completely inhibit the opening of NSCCs induced by ACh.

Figure 7. EAED blocks VDLCC and NSCC currents. (A) Protocol for measuring the VDLCC current of a single tracheal smooth muscle. (B) The VDLCC current was blocked by EAED or nifedipine under depolarized cell membrane conditions. (C) The I-V curve was plotted based on the experimental results of six different tracheal smooth muscle cells. (D) Protocol for recording NSCC currents in a single tracheal smooth muscle. (E) At −70 mV, point a is the NSCC state when K^+, Cl^-, and VDLCC currents are excluded under physiological conditions; point b is the NSCC opening after 100 μM ACh stimulation, reaching the plateau stage; point c is the state of NSCCs when 3.16 mg/mL EAED is added. (F) The broken-line diagram obtained by the experimental statistics of the net slope current at time points a, b, and c is based on Figure 6B. (G) The average currents for time points b and c at −70 mV (n = 6). ***P < 0.001.

The drug toxicity of EAED is very low at the tissue level

Next, the toxicity of EAED in mouse TRs was analyzed. After 3.16 mg/mL EAED completely blocked the contraction induced by ACh, the TRs were eluted and balanced for a period of time, again with ACh

stimulation, and the contraction apparently occurred again (Figure 8A). The second ACh-induced shrinkage was about 81% that of the first (Figure 8B). The above results showed that EAED had little effect on the activity of TRs when relaxing them and could be used in in vivo experiments.

Figure 8. TRs can still be stimulated to shrink after relaxation by EAED. (A) After 3.16 mg/mL EAED was added to inhibit the ACh-induced contraction, the TRs were stimulated to shrink again by ACh. (B) A comparison of contraction rates after the first and second ACh stimuli. The results were obtained from 6 TRs. ***P < 0.001.

EAED reduces the respiratory resistance induced by ACh in control and asthma groups

To investigate whether EAED could potentially improve airway hyperresponsiveness in mice, the lung functions of groups of healthy or asthmatic mice were assessed by the forced oscillation technique at baseline and after exposure to doubling concentrations of aerosolized ACh (3.125–50 mg/mL) dissolved with vehicle or EAED. Under baseline conditions, the four experimental groups studied were indistinguishable with the forced oscillation technique. When the ACh concentration was increased to 25–50 mg/mL, the atomized EAED dissolved with ACh significantly reduced the respiratory resistance of the control and asthma groups compared with the vehicle group (Figure 9). As expected, the asthmatic mouse group demonstrated ACh-sensitive hyperresponsiveness compared with the control group, particularly after the addition of 25 and/or 50 mg/mL aerosol ACh.

Figure 9. EAED reduces the respiratory resistance induced by ACh in control and asthma groups. At the baseline level (B), there was no significant difference in respiratory resistance between the four groups. When the ACh concentration was increased to 25–50 mg/mL, the atomized ACh dissolved with EAED significantly reduced the respiratory resistance of the control and asthma groups compared with the vehicle group. (*P < 0.05 Asthma+Vehicle vs Asthma+EAED, **P < 0.01 Asthma+Vehicle vs Control+Vehicle, #P < 0.05 Control+Vehicle vs Control+EAED; ANOVA).

Discussion

In this study, we found that EAED reduced both high K^+- and ACh-induced precontractions in mouse TRs and lung slices by inhibiting L-type Ca^{2+} channels and additional TRPC3 and/or STIM/Orai channels, respectively. EAED suppressed the cytoplasmic Ca^{2+} concentration elevation caused by high K^+ and ACh. In addition, in an in vivo study, EAED effectively reduced the elevated respiratory resistance, R_{rs}, induced by ACh in healthy and asthmatic mice.

As mentioned above, β2 adrenergic receptor agonists are often used as first-line bronchodilators to relieve asthma [23], but their use has been associated with many adverse effects and high recurrence rates. Thus, we aimed to identify bronchodilators derived from plants. We first extracted a component—EAED—from dandelion. To investigate whether EAED has a diastolic effect on the ASM of mice, two stimuli—high K^+ and ACh—were applied to elicit mouse TR precontractions and examine the effects of EAED. The

experimental results showed that EAED markedly antagonized both high K^+- and ACh-induced TR contractions in mice, with the maximum relaxant efficiency reaching almost 100% (Figures 1 and 2). These data demonstrated that EAED possesses relaxant potency against contractions induced by ACh/high K^+ stimulation.

We further investigated the underlying mechanism of the EAED-mediated relaxant effects on high K^+-induced contraction. The experiments were conducted under 0 and 2 mM extracellular Ca^{2+} conditions. High K^+ caused membrane depolarization, leading to the activation of VDLCCs [24]. In our study, high K^+-induced contractions were completely abolished in Ca^{2+}-free medium (Figure 5A), suggesting that this type of contraction may be dependent on Ca^{2+} influx through VDLCCs. Moreover, EAED completely blocked VDLCC currents (Figure 7A). These data indicated that EAED relaxed high K^+-induced contraction by blocking VDLCC-mediated Ca^{2+} influx (Figure 5A and B).

We then explored the pathways involved in EAED-mediated relaxation of ACh-induced contractions. We found that nifedipine partially inhibited ACh-induced sustained contractions under 2 mM Ca^{2+} conditions but had no effect on ACh-induced transient contractions under 0 Ca^{2+} conditions (Figures 4A and 5C). These results suggested that VDLCCs were responsible for the long-lasting contractions triggered by extracellular Ca^{2+} influx, but not intracellular Ca^{2+} release-induced transient contractions. However, EAED almost entirely eliminated both of these two types of contractions (Figure 5D), which suggests that the relaxant effects of EAED depend on blockade of both the extracellular Ca^{2+} influx-mediated by VDLCCs and the intracellular Ca^{2+} release.

Moreover, TRPC3 and/or STIM/Orai channels, as NSCCs, also play roles in ACh-induced contractions by mediating Ca^{2+} influx [25]. Our results indicate that Pyr3 can also cause partial inhibition in the presence of nifedipine, which proves that TRPC3 and/or STIM/Orai channels are also involved in the contraction process. In addition, the NSCC current was effectively blocked by EAED (Figure 7B). However, in addition to L-type Ca^{2+} channels and NSCCs, other channels may mediate the ACh-induced contractions further inhibited by EAED (Figure 4C). These unknown mechanisms require additional investigation.

The above experimental results were all obtained using the main trachea of mice. Moreover, our subsequent experiments conducted in lung slices suggested that EAED could also inhibit bronchial smooth muscle contraction (Figure 3), indicating that EAED is able to entirely block ASM contraction. In terms of Ca^{2+} dynamics in ASMCs, we further showed that EAED decreased high K^+- and ACh-mediated increases in intracellular Ca^{2+} (Figure 6). In addition, our in vivo work revealed that EAED could relieve respiratory resistance in healthy and asthmatic mice (Figure 9).

Conclusion

In summary, this study demonstrated that EAED inhibits agonist-induced sustained contractions of ASM by inhibiting several types of ion channels, decreases agonist-induced elevation of the cytosolic free Ca^{2+}

concentration in ASMCs, and relieves respiratory resistance in healthy and asthmatic mice. Meanwhile, unknown pathways might also be involved in EAED-mediated relaxation, in addition to VDLCCs and NSCCs. These results suggest that EAED could be a new inhibitor of asthma attacks.

Abbreviations

EAED: Ethyl acetate extract from Dandelion

ASM: Airway smooth muscle

ASMCs: Airway smooth muscle cells

FOT: Forced oscillation technique

TMHM: Taraxacum mongolicum Hand.-Mazz.

LPS: Lipopolysaccharide

ACH: Acetylcholine chloride

Pyr3: pyrazole3

SPF: Specific pathogen free

Rrs: Respiratory system resistance

Declarations

Ethics approval and consent to participate

All methods applied in this study are in accordance with protocols approved by the South-Central University for Nationalities. All mice animal experiments were approved and performed under the supervision of the Institutional Animal Care and Use Committee of the South-Central University for Nationalities.

Consent for publication

Not applicable.

Competing Interests

The authors declare no competing Interests.

Funding

The present study was financially supported by National Natural Science Foundation of China grants (31070744, 81573561 and 81774000), Fundamental Research Funds for the Central Universities, South-Central University for Nationalities (CZY20004, CZP17060 and CZP17048), Wuhan Applied Basic Research Program of Science and Technology (2017060201010217) and Fund for Key Laboratory Construction of Hubei Province (Grant No. 2018BFC360). The funders had no role in study design, data collection and analysis, decision to publish, or preparation of the manuscript.

Availability of data and materials

The data and materials supporting the conclusions are included within the article and its supplementary information files.

Authors' contributions

PZ and JL contributed equally to this study. PZ contributed to study design and guidance. JL conducted the experiments and wrote the manuscript. JWH and ZWY participated in scientific assistance. JPD provided Vibratome. DT and QM participated in data interpretation. JHS, QHL, PZ, and XZY supervised this study and edited the manuscript.

Acknowledgements

The authors gratefully acknowledge all the fellows in Institute for Medical Biology, College of Life Sciences, South-Central University for Nationalities.

References

1. O. Enilari and S. Sinha, The Global Impact of Asthma in Adult Populations, *Ann Glob Health*, 2019, **85**.
2. Z. C. Yang, Z. H. Qu, M. J. Yi, Y. C. Shan, N. Ran, L. Xu and X. J. Liu, MiR-448-5p inhibits TGF-beta1-induced epithelial-mesenchymal transition and pulmonary fibrosis by targeting Six1 in asthma, *J Cell Physiol*, 2019, **234**, 8804-8814.
3. C. J. Koziol-White and R. A. Panettieri, Jr., Modulation of Bronchomotor Tone Pathways in Airway Smooth Muscle Function and Bronchomotor Tone in Asthma, *Clin Chest Med*, 2019, **40**, 51-57.
4. J. M. Dai, K. H. Kuo, J. M. Leo, C. van Breemen and C. H. Lee, Mechanism of ACh-induced asynchronous calcium waves and tonic contraction in porcine tracheal muscle bundle, *American journal of physiology. Lung cellular and molecular physiology*, 2006, **290**, L459-469.
5. M. Gonzalez-Castejon, F. Visioli and A. Rodriguez-Casado, Diverse biological activities of dandelion, *Nutr Rev*, 2012, **70**, 534-547.
6. H. B. Wang, Cellulase-assisted extraction and antibacterial activity of polysaccharides from the dandelion Taraxacum officinale, *Carbohydr Polym*, 2014, **103**, 140-142.

7. L. Qian, Y. Zhou, Z. Teng, C. L. Du and C. Tian, Preparation and antibacterial activity of oligosaccharides derived from dandelion, *Int J Biol Macromol*, 2014, **64**, 392-394.
8. W. He, H. Han, W. Wang and B. Gao, Anti-influenza virus effect of aqueous extracts from dandelion, *Virol J*, 2011, **8**, 538.
9. G. Rehman, M. Hamayun, A. Iqbal, S. A. Khan, H. Khan, A. Shehzad, A. L. Khan, A. Hussain, H. Y. Kim, J. Ahmad, A. Ahmad, A. Ali and I. J. Lee, Effect of Methanolic Extract of Dandelion Roots on Cancer Cell Lines and AMP-Activated Protein Kinase Pathway, *Frontiers in pharmacology*, 2017, **8**, 875.
10. P. Ovadje, S. Ammar, J. A. Guerrero, J. T. Arnason and S. Pandey, Dandelion root extract affects colorectal cancer proliferation and survival through the activation of multiple death signalling pathways, *Oncotarget*, 2016, **7**, 73080-73100.
11. P. Ovadje, M. Chochkeh, P. Akbari-Asl, C. Hamm and S. Pandey, Selective induction of apoptosis and autophagy through treatment with dandelion root extract in human pancreatic cancer cells, *Pancreas*, 2012, **41**, 1039-1047.
12. P. Ovadje, S. Chatterjee, C. Griffin, C. Tran, C. Hamm and S. Pandey, Selective induction of apoptosis through activation of caspase-8 in human leukemia cells (Jurkat) by dandelion root extract, *Journal of ethnopharmacology*, 2011, **133**, 86-91.
13. L. T. Rahmat and L. E. Damon, The Use of Natural Health Products Especially Papaya Leaf Extract and Dandelion Root Extract in Previously Untreated Chronic Myelomonocytic Leukemia, *Case Rep Hematol*, 2018, **2018**, 7267920.
14. D. Jedrejek, B. Kontek, B. Lis, A. Stochmal and B. Olas, Evaluation of antioxidant activity of phenolic fractions from the leaves and petals of dandelion in human plasma treated with H2O2 and H2O2/Fe, *Chem Biol Interact*, 2017, **262**, 29-37.
15. A. Ding and X. Wen, Dandelion root extract protects NCM460 colonic cells and relieves experimental mouse colitis, *J Nat Med*, 2018, **72**, 857-866.
16. Q. Liu, H. Zhao, Y. Gao, Y. Meng, X. X. Zhao and S. N. Pan, Effects of Dandelion Extract on the Proliferation of Rat Skeletal Muscle Cells and the Inhibition of a Lipopolysaccharide-Induced Inflammatory Reaction, *Chin Med J (Engl)*, 2018, **131**, 1724-1731.
17. C. Ma, L. Zhu, J. Wang, H. He, X. Chang, J. Gao, W. Shumin and T. Yan, Anti-inflammatory effects of water extract of Taraxacum mongolicum hand.-Mazz on lipopolysaccharide-induced inflammation in acute lung injury by suppressing PI3K/Akt/mTOR signaling pathway, *Journal of ethnopharmacology*, 2015, **168**, 349-355.
18. N. Yang, C. Li, G. Tian, M. Zhu, W. Bu, J. Chen, X. Hou, L. Di, X. Jia, Z. Dong and L. Feng, Organic acid component from Taraxacum mongolicum Hand.-Mazz alleviates inflammatory injury in lipopolysaccharide-induced acute tracheobronchitis of ICR mice through TLR4/NF-kappaB signaling pathway, *Int Immunopharmacol*, 2016, **34**, 92-100.
19. N. Yang, Z. Dong, G. Tian, M. Zhu, C. Li, W. Bu, J. Chen, X. Hou, Y. Liu, G. Wang, X. Jia, L. Di and L. Feng, Protective effects of organic acid component from Taraxacum mongolicum Hand.-Mazz.

against LPS-induced inflammation: Regulating the TLR4/IKK/NF-kappaB signal pathway, *Journal of ethnopharmacology*, 2016, **194**, 395-402.

20. J. Liu, H. Xiong, Y. Cheng, C. Cui, X. Zhang, L. Xu and X. Zhang, Effects of taraxasterol on ovalbumin-induced allergic asthma in mice, *Journal of ethnopharmacology*, 2013, **148**, 787-793.
21. Q. R. Tuo, Y. F. Ma, W. Chen, X. J. Luo, J. Shen, D. Guo, Y. M. Zheng, Y. X. Wang, G. Ji and Q. H. Liu, Reactive oxygen species induce a Ca(2+)-spark increase in sensitized murine airway smooth muscle cells, *Biochem Biophys Res Commun*, 2013, **434**, 498-502.
22. Y. S. She, L. Q. Ma, B. B. Liu, W. J. Zhang, J. Y. Qiu, Y. Y. Chen, M. Y. Li, L. Xue, X. Luo, Q. Wang, H. Xu, D. A. Zang, X. X. Zhao, L. Cao, J. Shen, Y. B. Peng, P. Zhao, M. F. Yu, W. Chen, X. Nie, C. Shen, S. Chen, S. Chen, G. Qin, J. Dai, J. Chen and Q. H. Liu, Semen cassiae Extract Inhibits Contraction of Airway Smooth Muscle, *Frontiers in pharmacology*, 2018, **9**, 1389.
23. A. Fust and N. L. Stephens, Relaxation of canine airway smooth muscle, *Can J Physiol Pharmacol*, 2007, **85**, 672-678.
24. T. Kirschstein, M. Rehberg, R. Bajorat, T. Tokay, K. Porath and R. Kohling, High K+-induced contraction requires depolarization-induced Ca2+ release from internal stores in rat gut smooth muscle, *Acta Pharmacol Sin*, 2009, **30**, 1123-1131.
25. M. Y. Wei, L. Xue, L. Tan, W. B. Sai, X. C. Liu, Q. J. Jiang, J. Shen, Y. B. Peng, P. Zhao, M. F. Yu, W. Chen, L. Q. Ma, K. Zhai, C. Zou, D. Guo, G. Qin, Y. M. Zheng, Y. X. Wang, G. Ji and Q. H. Liu, Involvement of large-conductance Ca2+-activated K+ channels in chloroquine-induced force alterations in pre-contracted airway smooth muscle, *PLoS One*, 2015, **10**, e0121566.

Figures

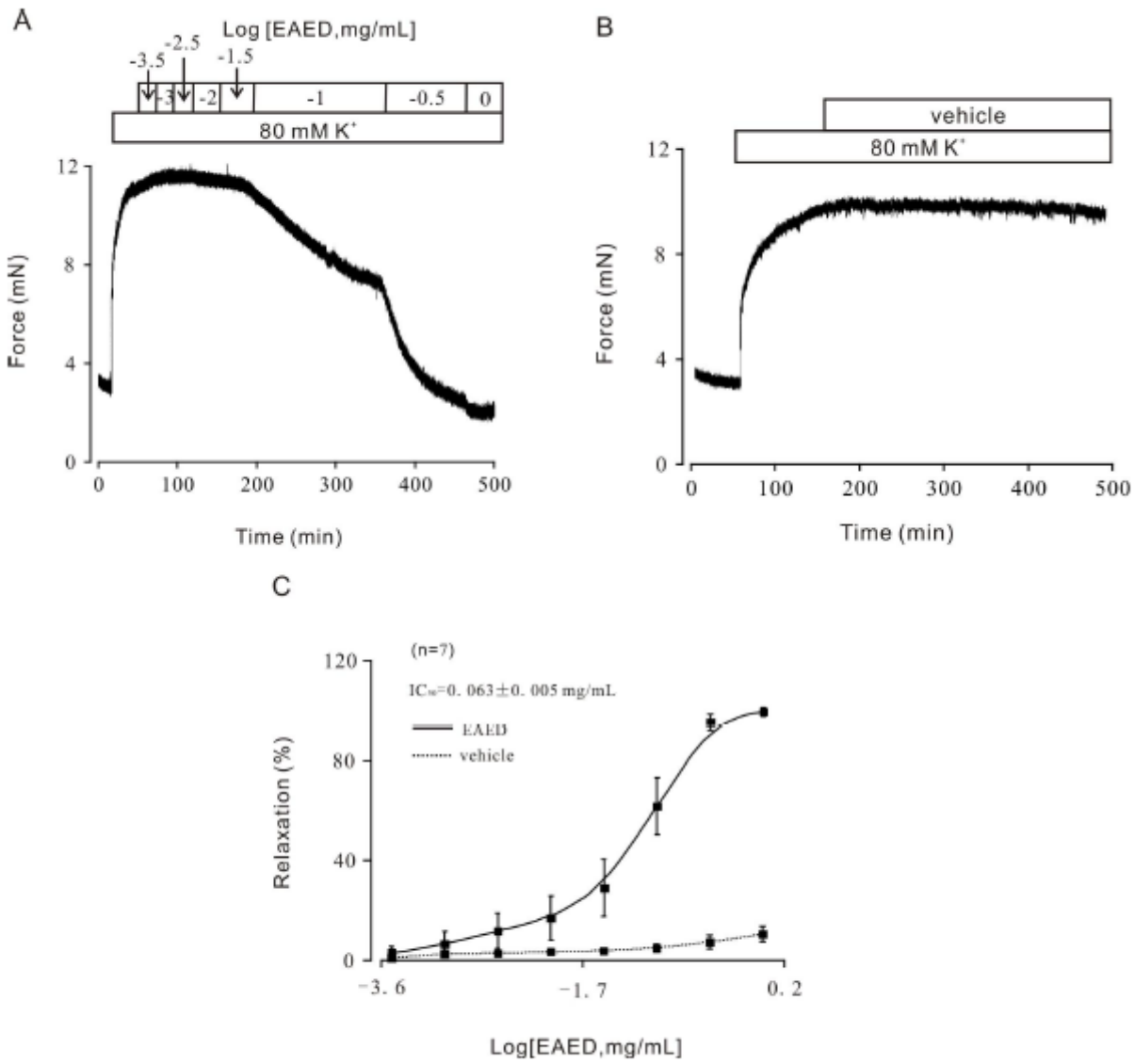

Figure 1

EAED inhibited high K+-induced tracheal ring contraction.

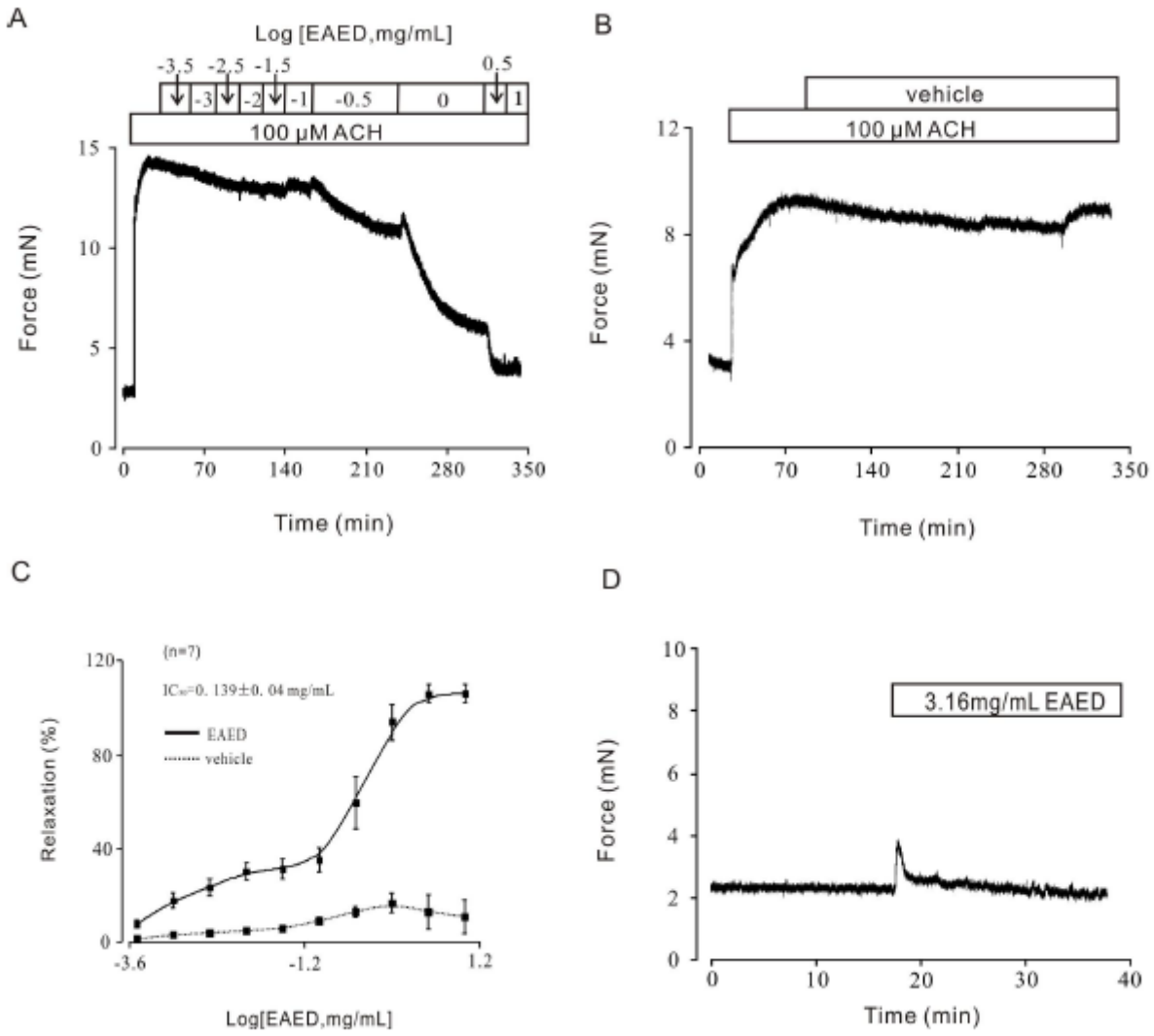

Figure 2

Contraction induced by ACH was inhibited by cumulative addition of EAED.

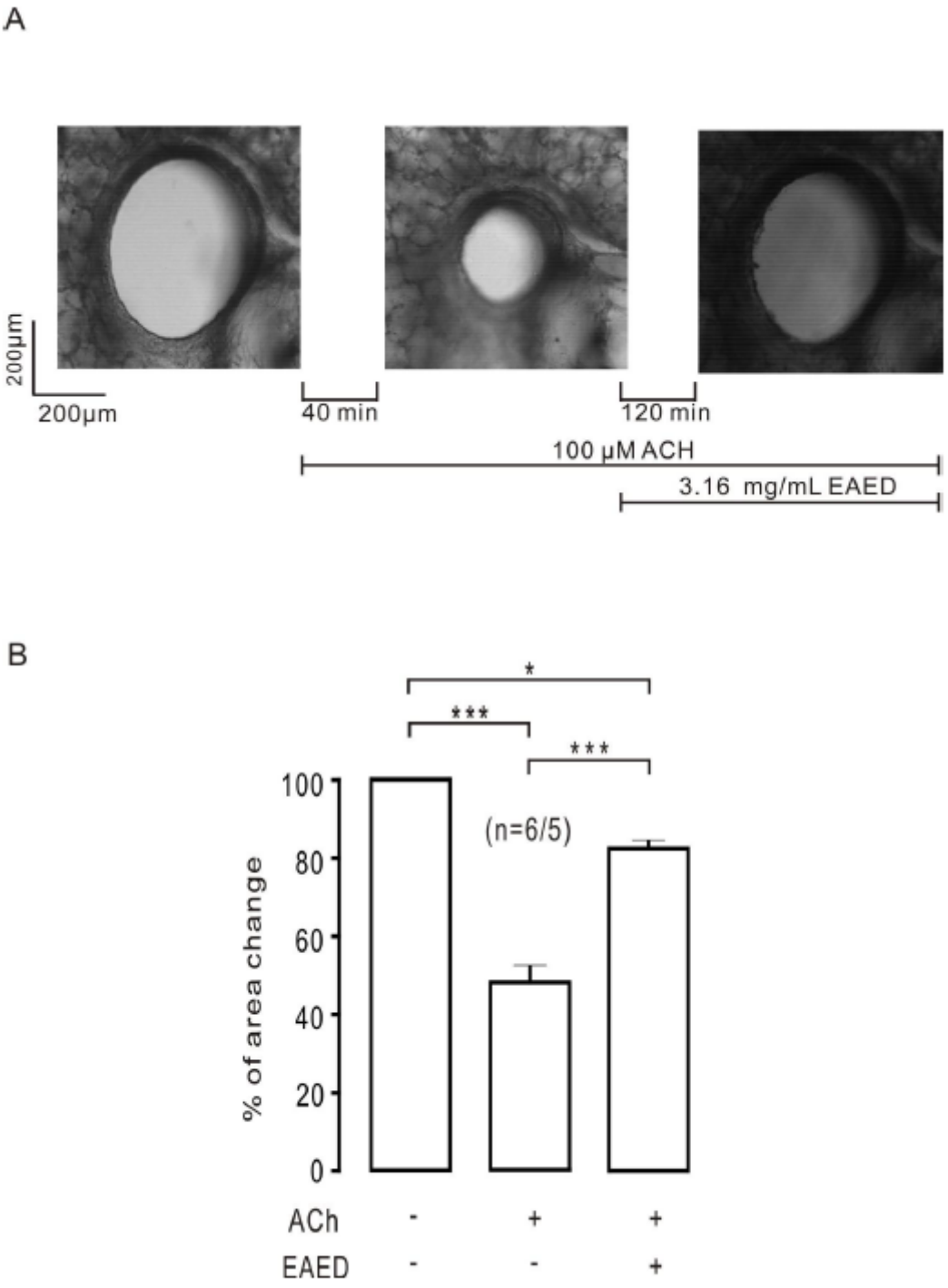

Figure 3

EAED inhibits contraction in lung slices.

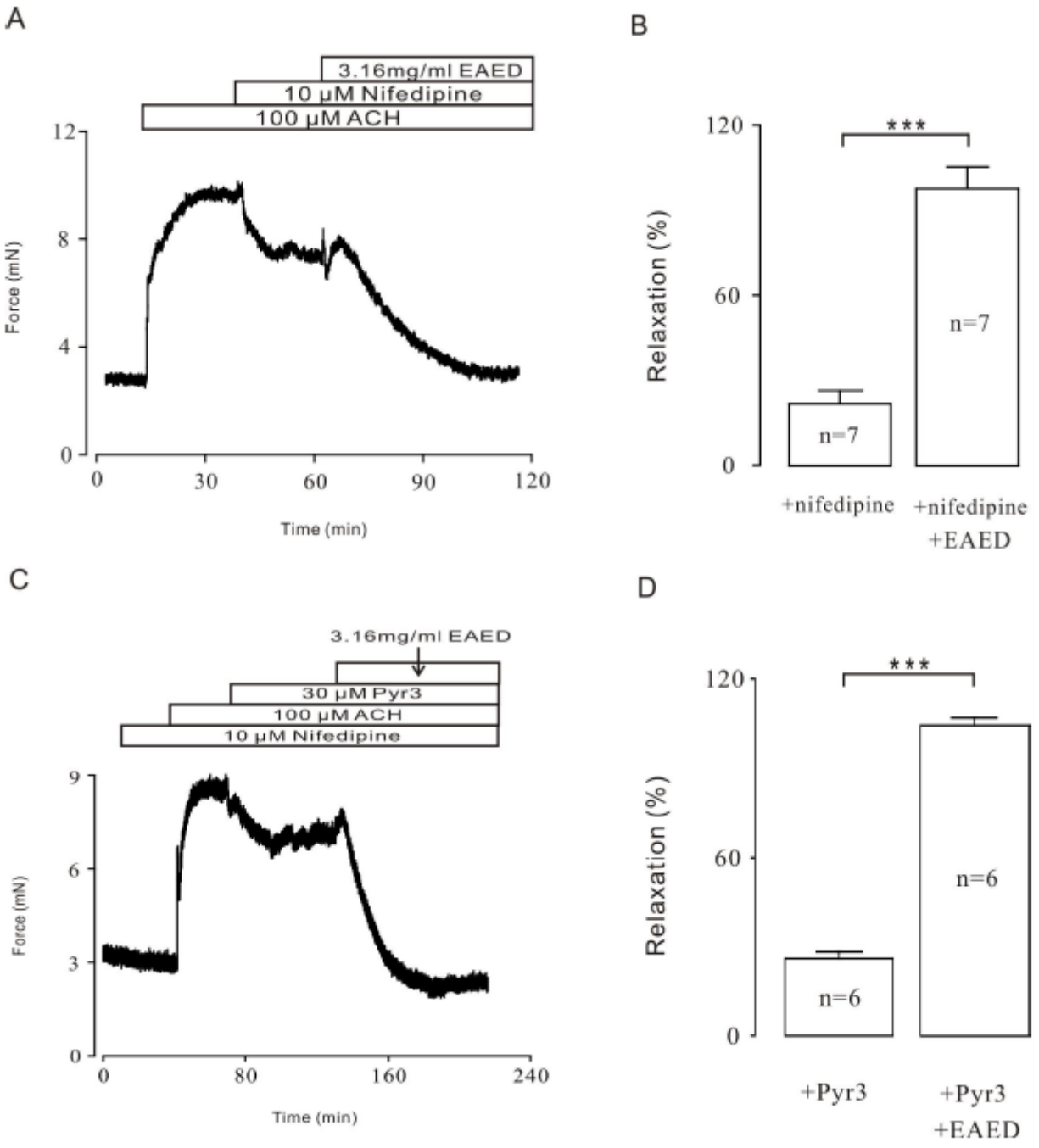

Figure 4

Nifedipine, Pyr3 partially inhibits ACH-induced contraction, respectively.

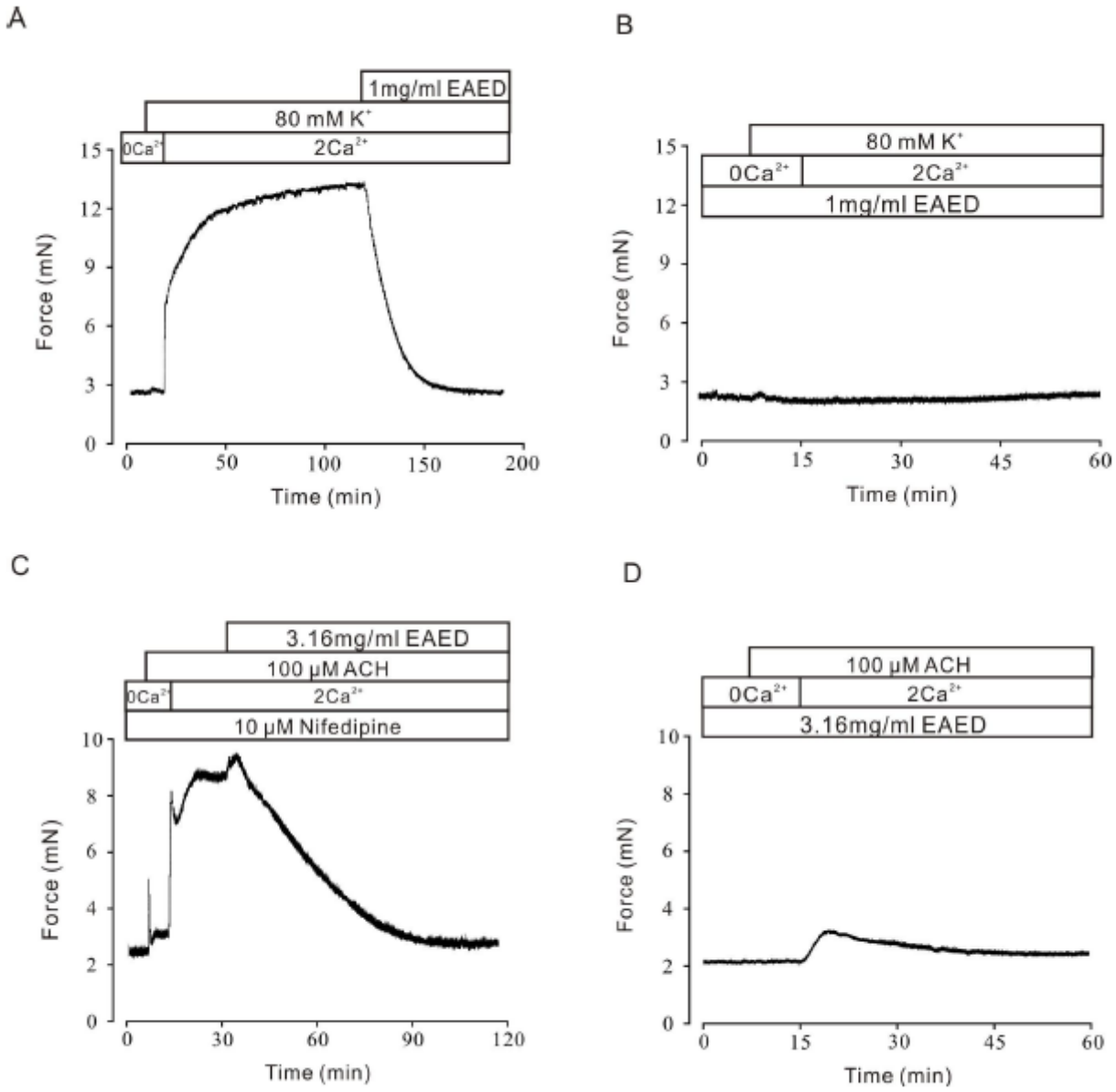

Figure 5

EAED blocks high K+-evoked Ca2+ influx and ACH-elicited Ca2+ influx and Ca2+ release.

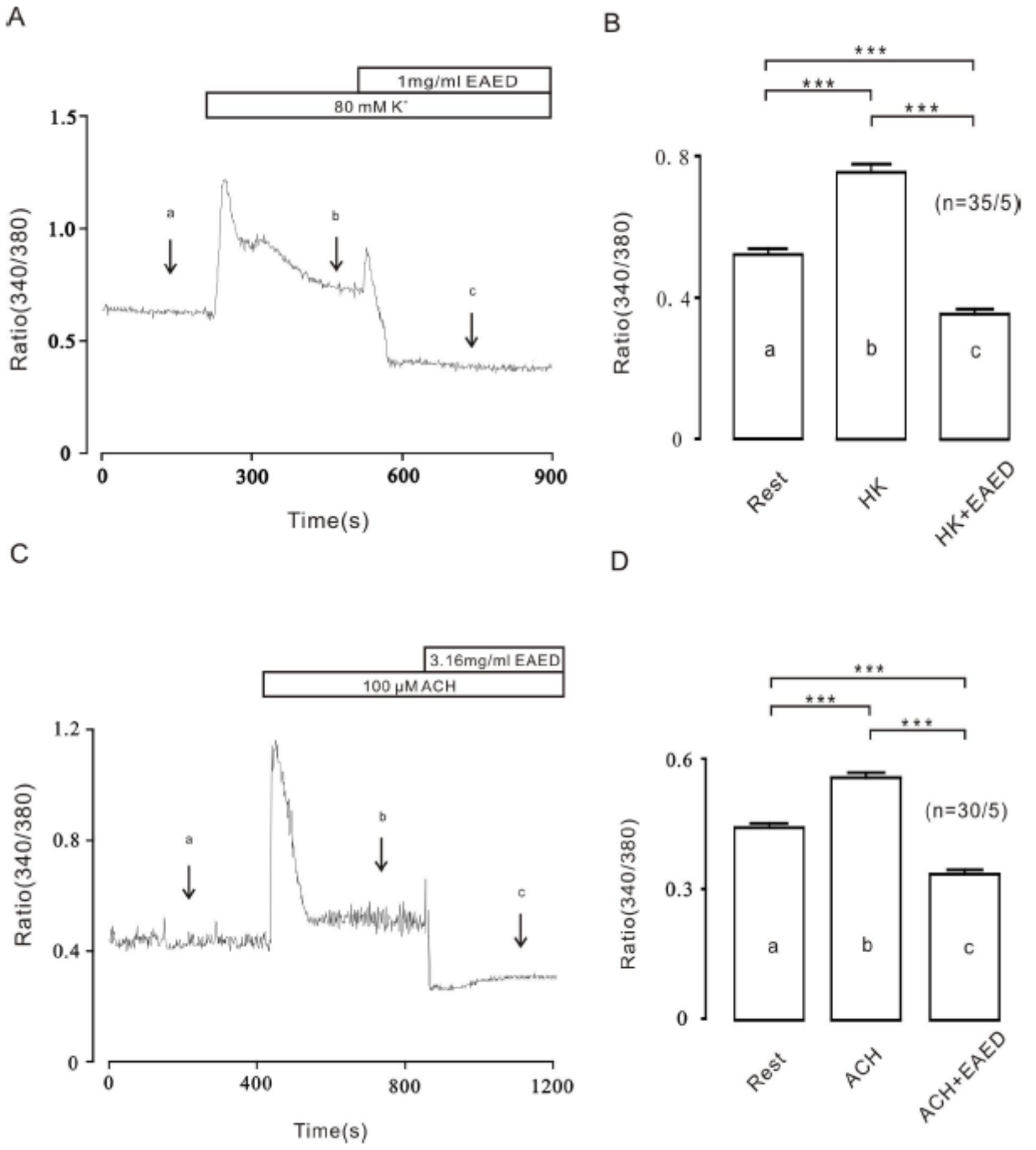

Figure 6

EAED inhibits high K+ and ACH-induced Ca2+ increases in single tracheal smooth muscle cells.

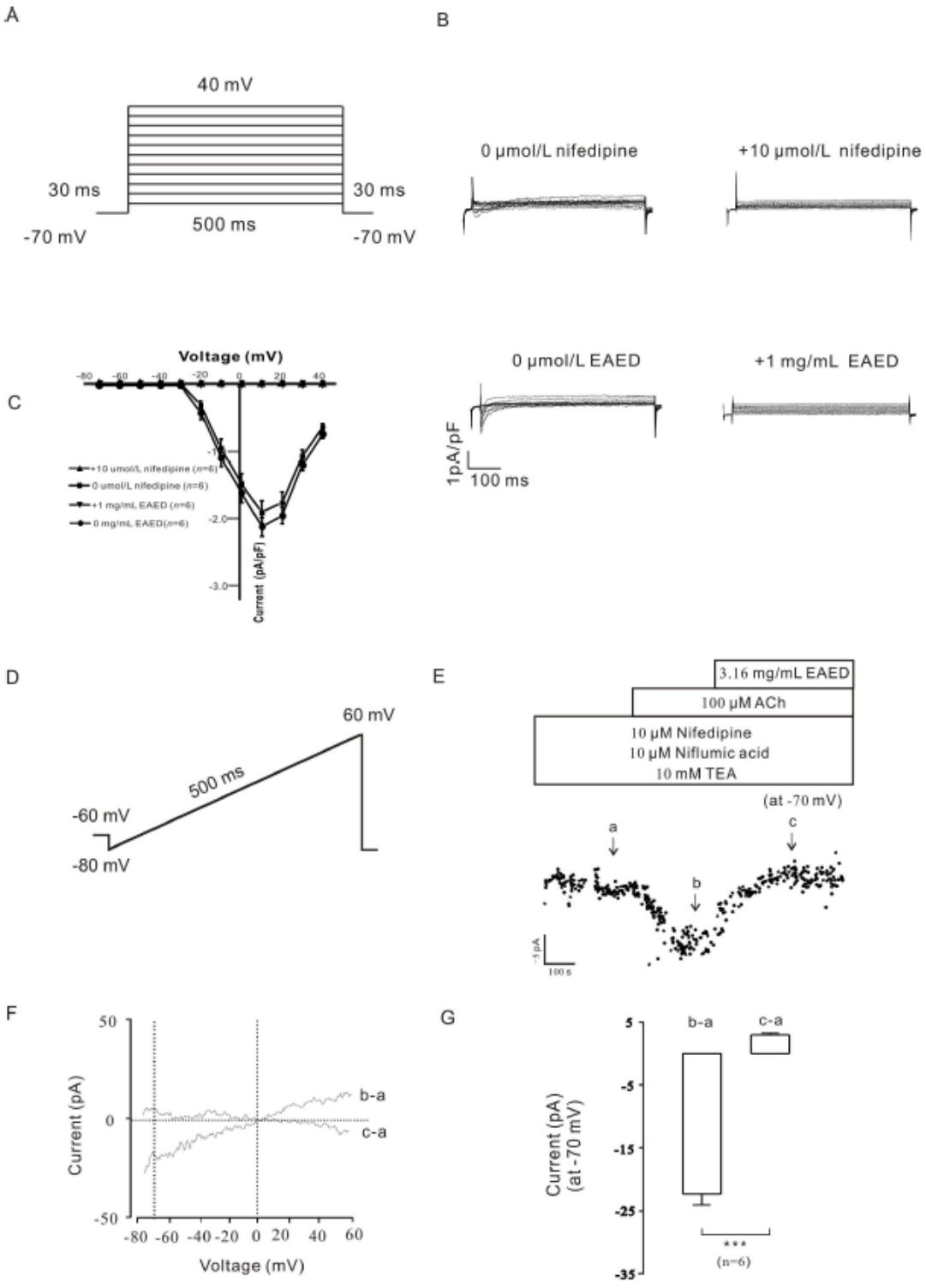

Figure 7

EAED blocks VDLCCs and NSCCs currents.

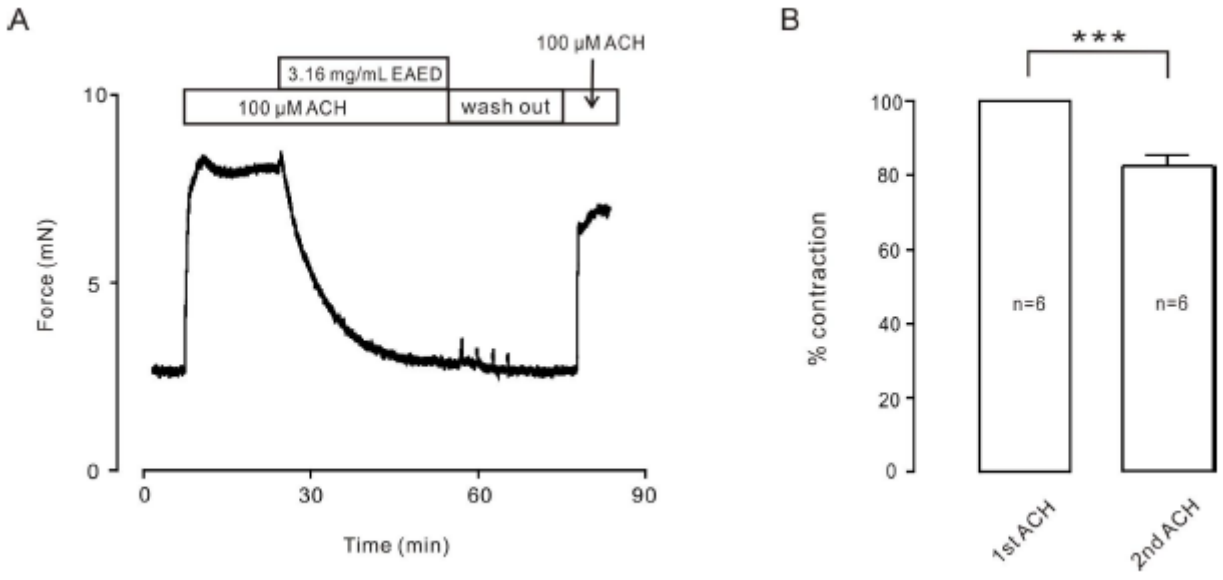

Figure 8

The tracheal rings could still be stimulated to shrink after relaxation by EAED.

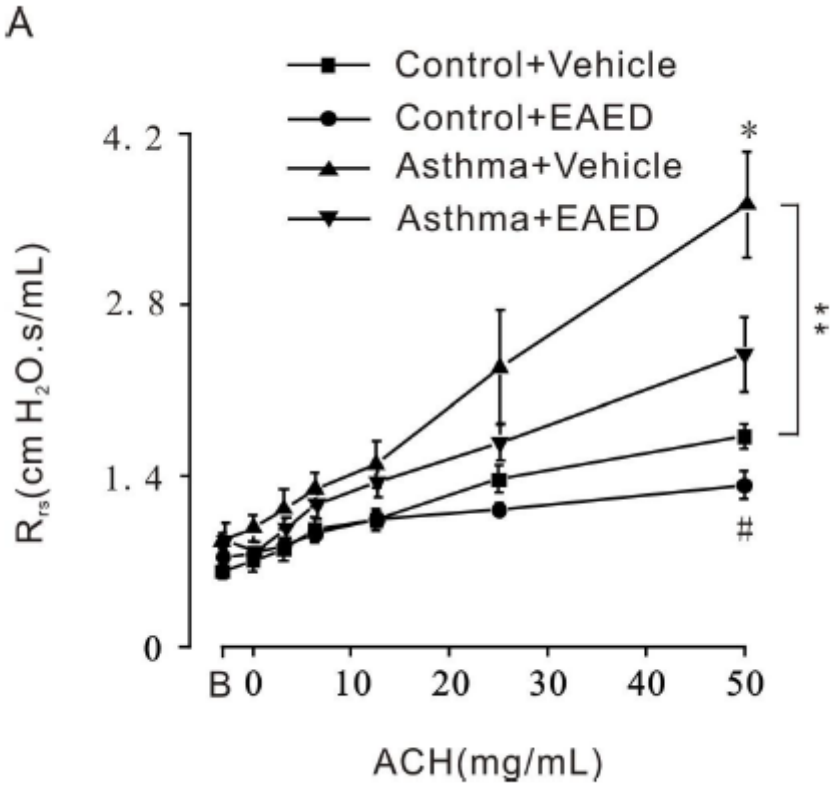

Figure 9

EAED reduced the respiratory resistance induced by ACH in the control group and the asthma group.